Submit to Biorxiv

Title: LrhA promotes CRISPR-Cas immunity by promoting reciprocal interplay between interference and primed adaptation in *Escherichia coli*

Running Title: LrhA coordinates CRISPR adaptation and interference in *E. coli*

Mengdie Fang [1,2], Na Li [1], Mingyue Fei [1], Yanan Lu [1], Mingjing Yu [1], Dongchang Sun [1*]

[1] College of Biotechnology and Bioengineering, Zhejiang University of Technology, Hangzhou, Zhejiang, 310014, China

[2] School of Laboratory Medicine and Bioengineering, Hangzhou Medical College, Hangzhou, Zhejiang, 310013, China

[*] Corresponding authors: sundch@zjut.edu.cn

Tel/Fax: +86 0571 88320057

ABSTRACT

The CRISPR-based defense system protects prokaryotes against invading plasmids and viruses by memorizing their nucleotide-sequence traits (adaptation) and destructing the nucleic acids (interference). Previous studies have indicated that CRISPR-Cas adaptive immunity is the outcome of the combined effect of adaptation and interference, but the environmental and physiological cues that coordinate these two processes are unclear. Here, we identify the LysR-type transcriptional regulator LrhA as an important CRISPR-Cas regulator, which promotes the clearance of CRISPR-targeted plasmid more efficiently at 37 ℃ than at 30 ℃ in *Escherichia coli*, by increasing the acquisition of new spacers via interference-driven adaptation. LrhA directly binds to the promoter of the *cas* operon to activate the transcription of *cas* genes required for adaptation and interference, thereby enhancing the CRISPR-Cas adaptive immunity. Altogether, our results demonstrate that LrhA plays a pivotal role in coordinating CRISPR adaptation and interference at the body temperature in a gut-dwelling bacterium.

42 ## INTRODUCTION

43 Prokaryotes have evolved diverse defense systems against plasmids and viruses.
44 Among them, the CRISPR-Cas adaptive immune system provides bacteria and
45 archaea with acquired and inheritable immunity against previously encountered
46 invading nucleic acids[1-6]. The CRISPR-Cas system acts in three distinct stages.
47 During the first contact with a foreign genetic element, short DNA fragments from
48 this element are incorporated into the CRISPR array, which contains the genetic
49 memory of previous infecting elements[7-9]. The incorporation of a new spacer derived
50 from the foreign DNA together with an additional repeat leads to the expansion of the
51 size of the CRISPR array. This process is termed adaptation[10-13]. Triggered by
52 environmental and physiological cues, Cas proteins are expressed, accompanied by
53 the transcription of the CRISPR array, and subsequent processing of the premature
54 CRISPR RNA (pre-crRNA) into mature crRNAs[14,15]. In the final stage termed
55 interference, crRNAs guide Cas proteins to the target sequence, where the Cas3
56 nuclease is recruited for cleaving the previously encountered foreign DNA[16,17]. Native
57 CRISPR-Cas systems have been engineered for broad applications such as genome
58 editing tools[18-21] and antimicrobials for combating multi-drug resistant (MDR)
59 bacteria [22-27]. Given that delivering engineered CRISPR-Cas systems as antimicrobials
60 in the form of DNA could be challenged by endogenous CRISPR-Cas systems, it is
61 critical to understand how the endogenous CRISPR-Cas systems are activated.

62 CRISPR-Cas adaptive immunity represents a powerful weapon of defense
63 in prokaryotes. On the other hand, invasive nucleic acids often rapidly evolve
64 resistance to CRISPR immunity by mutating the CRISPR-targeted region. To fight
65 back, a process named 'primed adaptation' is provoked to rapidly incorporate new
66 spacers, derived from DNA fragments produced by interference, for upgrading the
67 CRISPR-Cas adaptive immunity[28-30]. Primed adaptation requires all components of
68 the CRISPR-Cas system for assembly of the interference and the adaptation
69 complexes[28,31]. Nevertheless, a high level of CRISPR-Cas adaptive immunity
70 increases the burden of producing Cas proteins and crRNAs, as well as the risk of

71 suicide from autoimmunity[32-35]. To finely tune the CRISPR immunity to a moderate
72 level, interference and adaptation are often inversely correlated: an intermediate level
73 of interference allows invasive nucleic acids to persist longer, leading to higher levels
74 of adaptation (interference-driven adaptation), while a strong interference leads to a
75 relatively low level of adaptation [36-38]. Although the working mechanisms of CRISPR
76 adaptation and interference have been intensively investigated[7,10,12,13,31,39-46], little is
77 known about environmental and physiological cues that adjust the CRISPR-Cas
78 adaptive immunity by leveraging both CRISPR interference and adaptation[14,15].
79 The type I CRISPR-Cas system, comprised of the multi-subunit RNA-guided
80 surveillance complex, the Cas3 nuclease, and the Cas1-Cas2 integrase, is most
81 prevalent in prokaryotes[47]. Regulation studies have focused on type I CRISPR-Cas
82 systems, especially the type I-E CRISPR-Cas system of *Escherichia coli*, in which
83 transcription of *cas* genes are positively regulated by the LysR type transcriptional
84 regulator (LTTR) LeuO[48] and the histone-like protein StpA[49,50], and negatively
85 controlled by the carbon catabolite regulator CRP[51] and the histone-like protein
86 H-NS[52]. Because the nuclease activity of Cas3, a limiting factor of CRISPR-Cas
87 interference, is low at the body temperature (i.e., 37 ℃)[53,54], previous studies have
88 been predominantly performed at the environmental temperature (i.e., 30 ℃) in *E.*
89 *coli*[50,52,55]. However, it remains unclear how the CRISPR-Cas system is activated at
90 the physiological temperature (37 ℃) in *E. coli*.
91 To study the regulation of the CRISPR-Cas adaptive immunity in *E. coli* at
92 physiological temperature, we screened for regulators of the CRISPR-Cas system at
93 37 ℃ by combining DNA pull-down and mass spectrometry, and identified the LTTR
94 protein LrhA as an important regulator. By promoting a positive feedback circuit
95 between interference and adaptation, LrhA augmented the clearance of
96 CRISPR-targeted plasmid at 37 ℃, via direct binding to the promoter of the *cas*
97 operon to stimulate the transcription of *cas* genes required for both adaptation and
98 interference. Our work uncovers a novel mechanism by which a bacterium
99 coordinates interference and adaptation to achieve optimal immunity in response to
100 temperature, providing a foundation for curbing the endogenous CRISPR-Cas system

101 when using CRISPR-Cas antimicrobials in different scenarios.

102 # RESULTS

103 ## Screening for proteins binding to the promoter of *cas* genes

104 Transcription of all *cas* genes except for *cas3* starts from the promoter P_{cas} upstream
105 of the *cas* operon[52] (Fig. 1a). Both H-NS and LeuO regulates the expression of the *cas*
106 operon by binding to specific sites within P_{cas} [48,52] (Fig. 1b, Supplementary Fig. S1).
107 To screen for regulators that potentially affect the transcription of *cas* genes at 37 ℃,
108 we performed a DNA pull-down assay using a DNA probe containing P_{cas} as a bait
109 (Fig. 1c). Because H-NS binds to high-affinity sites within P_{cas} and spreads along the
110 adjacent DNA[56], potentially masking the binding sites of other regulators, we
111 screened for proteins binding to P_{cas} in *hns*-deletion mutants of two *E. coli* strains
112 (MC4100 and BW25113). Mass spectrometry analysis showed that more than one
113 hundred proteins in each strain were isolated with the biotinylated P_{cas}
114 (Supplementary Fig. S2a). Among them, 49 proteins were detected in both strains
115 (Supplementary Fig. S2b, Supplementary Table S1). According to the bioinformatic
116 analysis of proteins with high coverage of matched peptides, 18 proteins were
117 classified as transcriptional factors (TFs), and 2 proteins (NadR and GlpR) were
118 annotated as multifunctional proteins (Supplementary Table S2). Two previously
119 documented regulators of the CRISPR-Cas system (i.e. StpA[49,50] and SlyA[57,58]) were
120 identified in the protein mixture bound to $P_{cas,}$ indicating that the screening approach
121 was effective. Remarkably, the LTTR LrhA was detected in protein mixtures bound to
122 P_{cas} in both strains (Fig. 1d, Supplementary Table S2), with high coverage of peptide
123 sequences (Fig. 1e, Supplementary Fig. S3). Subsequent pull-down assay confirmed
124 that purified LrhA with a 6×His-tag bound $P_{cas,}$ indicating that LrhA is a potential
125 regulator of the CRISPR-Cas system in *E. coli* (Fig. 1f).

126 To check whether P_{cas}-binding TFs regulate transcription of the *cas* operon, their
127 effects on the activity of P_{cas} were evaluated with a previously described fluorescence
128 reporter system[50] (Fig. 1g upper panel). To avoid the effect of the known strong
129 regulators H-NS and LeuO, the 12 predicted TFs, and LeuO (as the positive control),

130 were separately over-expressed in an Δ*hns* Δ*leuO* mutant. SlyA promoted the activity
131 of P_{cas} by 2.4-fold (Fig. 1g), in agreement with the previous report [59]. Eight TFs
132 contain the HTH-type DNA binding domain, which is also present in LeuO (Fig. 1h).
133 The LTTR ArgP, known to act either as transcriptional activators or repressors
134 depending on its binding with two effectors lysine and arginine[60], reduced the activity
135 of P_{cas} by 70%, while LrhA increased the activity of P_{cas} by more than 2-fold (Fig. 1g).
136 Although YdcI and AaeR also belong to LTTRs and bind to P_{cas}, they showed
137 minimal (if any) effect on the activity of P_{cas} (Fig. 1g). Overexpression of the glycerol
138 metabolic regulator GlpR also resulted in strong stimulation of the transcription of
139 P_{cas}, increasing their transcripts by more than 2 folds (Fig. 1g). Thus, we narrowed
140 down to the regulators LrhA, ArgP, GlpR and SlyA below.

141 **Activation of clearance of the CRISPR-targeted plasmid by LrhA is affected by**
142 **temperature**

143 We investigated the function of LrhA, ArgP, GlpR and SlyA on CRISPR interference
144 by examining clearance of the CRISPR-targeted plasmid (pT) and the
145 CRISPR-non-targeted plasmid (pNT) in the Δ*hns* Δ*leuO* mutant at 37 ℃ (Fig. 2a). As
146 shown in Fig. 2b, overexpression of LrhA promoted the clearance rates of the pT but
147 not the pNT after 24h growth, while overexpression of SlyA or ArgP did not affect
148 the clearance rates of both plasmids. Overexpression of GlpR reduced cell viability to
149 a similar level regardless of the harboring plasmids, but showed no effect on CRISPR
150 interference (Fig. 2b). Therefore, we focused on LrhA in the following investigation.
151 To confirm the impact of LrhA on the CRISPR system, a *lrhA*$^-$ strain was generated
152 by in-frame deletion of *lrhA* in the Δ*hns* Δ*leuO* mutant, and the clearance of the pT
153 was determined in this mutant. The *lrhA*$^-$ strain formed swarm rings with increased
154 diameter compared with the *lrhA*$^+$ strain (Supplementary Fig. S4), in agreement with
155 the previous report that LrhA represses transcription of the motility master regulator
156 operon *flhDC*[61]. Activation of CRISPR interference by LrhA was examined with the
157 pT and the pNT, through a documented natural transformation method[50,62-64] and
158 plasmid loss in transformants. Although the ratios of transformation efficiencies

159 (pT/pNT) were similar in *lrhA*$^{+}$ and *lrhA*$^{-}$ mutants (Supplementary Fig. S5a), stability
160 of the pT varied in transformants which were grown in test tubes with antibiotic-free
161 LB medium at 37℃ and at 30 ℃. The clearance rate of the pT in the *lrhA*$^{+}$ strain was
162 decreased faster than in the *lrhA*$^{-}$ strain (Supplementary Fig. S5b). After 36 h
163 incubation, the clearance rate of the pT was more than 12-fold lower at 37 ℃ while
164 only 5-fold at 30 ℃ in the *lrhA*$^{-}$ strain than in the *lrhA*$^{+}$ strain (Fig. 2c).
165 Complementing *lrhA* on genome (*lrhA*^{c}) partially regained the CRISPR interference at
166 both 37 ℃ and 30 ℃ (Fig. 2c-d). These results indicate that LrhA activates CRISPR
167 interference and the impact of LrhA on CRISPR interference is
168 temperature-dependent, stronger at 37 ℃ than at 30 ℃.

169 **Promotion of the primed adaptation by LrhA is affected by temperature**

170 In contrast to the naïve adaptation which requires only the Cas1-Cas2 integrase, all
171 components of the CRISPR-Cas system are involved in the acquisition of DNA
172 spacers from CRISPR-targeted DNA during the primed adaptation[10,11,13,65]. To
173 investigate the role of LrhA in adaptation, we monitored CRISPR array expansion in
174 response to the pT and the pNT in *lrhA*$^{+}$ and *lrhA*$^{-}$ strains (Fig. 2e). Compared with
175 that in the *lrhA*$^{+}$ strain, fewer expansion events were observed in the *lrhA*$^{-}$ mutant
176 carrying the CRISPR targeted plasmid after 1.5 or 3 days of incubation at 30 ℃ and
177 37 ℃ (Fig. 2f, Supplementary Fig. S6a). CRISPR array expansion was not observed
178 in the *lrhA*$^{+}$ and *lrhA*$^{-}$ strains carrying the pNT, or in the strains lacking the *cas*
179 operon (Fig. 2f, Supplementary Fig. S6b), indicating that LrhA promotes the primed
180 but not the naïve adaptation.

181 Consistent with a stronger impact of LrhA on CRISPR interference at higher
182 temperature, the expansion band of the CRISPR array from the *lrhA*$^{+}$ strain was more
183 evident at 37 ℃ than at 30 ℃ (Fig. 2e, Supplementary Fig. S6a), suggesting that
184 acquisition of new spaces occurred more frequently when LrhA was expressed at the
185 body temperature. Complementing *lrhA* on the genome of the *lrhA*$^{-}$ mutant (*lrhA*^{c})
186 restored adaptation at 37 ℃, but the restoration effect was weaker at 30 ℃
187 (Supplementary Fig. S6a). Sequencing analysis of the expansion bands revealed that
188 all newly formed spacers (20/20) were derived from the CRISPR targeted plasmid

189 (Fig. 2g), with a strong preference for an AAG PAM (16/20) during adaptation, and a
190 pronounced bias in the DNA strand (15/20) matching the orientation of the
191 CRISPR-targeting units (CR1) (Supplementary Table S3), in agreement with typical
192 traits of primed CRISPR adaptation[28,30].

193 **Cas1-2 is essential to activation of CRISPR interference by LrhA**

194 LrhA promoted CRISPR-Cas interference and adaptation over a period of days more
195 efficiently at 37 ℃ than at 30 ℃ (Fig. 2). Because acquisition of new spacers allows
196 bacteria to mount more efficient CRISPR interference[28,30,66], we hypothesized that
197 high CRISPR-Cas interference and adaptation were coupled and reinforced by LrhA
198 at 37 ℃. To test this, we deleted both *cas1* and *cas2* (Δ*cas1-2*) in *lrhA*$^+$ and *lrhA*$^-$
199 strains, and examined the CRISPR interference in the two strains through the plasmid
200 loss assay. *cas1-cas2* deletion abolished the CRISPR array expansion at both 37 ℃
201 and 30 ℃ (Fig. 2j), consistent with their critical role in adaption. Strikingly, the
202 clearance rates of the pT in the *lrhA*$^+$ mutant with *cas1-cas2* deletion were similarly
203 low at 37 ℃ and 30 ℃ (Fig. 2h-i), indicating that the temperature effect on
204 LrhA-promoted interference disappeared when adaptation was abolished. In addition,
205 *cas1-cas2* deletion reduced the effect on LrhA in CRISPR interference activity at both
206 37 ℃ and 30 ℃ (Fig. 2h-i), indicating that LrhA contributes to the positive feedback
207 of interference and adaptation process (Fig. 2k).

208 **LrhA activates transcription of the *cas* operon**

209 To understand how LrhA controls the CRISPR-Cas adaptive immunity, its role in
210 regulating the *cas* operon was evaluated with a previously documented reporter
211 system. We detected only a subtle effect of chromosomally expressed LrhA on the
212 activity of P_{cas}. Although *lrhA* inactivation decreased the activity of P_{cas} by 31% and
213 37% in the Δ*hns* Δ*leuO* mutant grown at 30 ℃ and 37 ℃, respectively,
214 complementing *lrhA* fully restored the activity of P_{cas} at 37 ℃, but only partially
215 restored it at 30 ℃ (Fig. 3a). A more pronounced effect of temperature on the activity
216 of P_{cas} was detected when LrhA was overexpressed. Expressing LrhA from an
217 arabinose-inducible promoter on a multi-copy plasmid elevated transcription of the
218 *cas* operon by 4.75 folds in the Δ*hns* Δ*leuO* mutant after 36 h of incubation at 37 ℃

219 (Fig. 3b middle panel). However, no significant effect of expressing LrhA on
220 transcription of the *cas* operon was observed when the Δ*hns* Δ*leuO* mutant was grown
221 at 30 ℃ (Fig. 3b left panel), indicating that the impact of LrhA on the transcription of
222 the *cas* operon was temperature-dependent. Interestingly, deletion of *lrhA* did not
223 affect the activity of P_{cas} in the Δ*hns* mutant grown at 30 ℃ and 37 ℃ (Fig. 3c). Also,
224 over-expressing LrhA in the Δ*hns* mutant only slightly increased transcription of the
225 *cas* operon after incubation for 36 h at 37 ℃, but not at 30 ℃ (Supplementary Fig.
226 S7a). In the wild-type strain, overexpressing LrhA did not affect the activity of P_{cas} at
227 either 30 ℃ or 37 ℃ (Supplementary Fig. S7b), revealing that the effect of LrhA on
228 the expression of the *cas* operon was masked by H-NS and LeuO, and implicating the
229 presence of a hierarchical regulation of the *cas* operon.

230 **LrhA activates the *cas* operon by directly binding to the promoter P_{cas}**

231 The LrhA-binding site was reported to partially overlap with a LeuO-binding site on
232 the promoter of *leuO*[67]. Previous work has identified two LeuO binding sites (LBS I
233 and LBS II) within P_{cas} (Supplementary Fig. S1). The observation that the presence of
234 LeuO interfered with the regulation of P_{cas} by LrhA prompted us to consider whether
235 LrhA and LeuO compete for the same binding sites on P_{cas}. To check this, DNA
236 probes lacking LBS I and/or LBS II were generated (named 'P_{cas} del LBS I', 'P_{cas} del
237 LBS II', and 'P_{cas} del LBS I&II') and EMSA was employed to determine the effect of
238 LBSI and LBS II on the efficiency of LrhA binding to P_{cas}. As shown in Fig. 4a, 700
239 nM of His-LrhA was sufficient to retard the mobility of the full-length P_{cas} probe (P_{cas}
240 FL). However, 2800 nM of His-LrhA were required to completely retard the
241 migration of the P_{cas} del LBS I and the P_{cas} del LBS II probes, respectively (Fig. 4a).
242 Particularly, in the absence of both LBSI and LBSII (P_{cas} del LBS I&II), more than
243 5600 nM of His-LrhA was necessary to saturate the binding of the probe. These
244 observations support that LrhA binds to both LBS I and LBS II. To confirm LBS I
245 and LBS II as binding sites of LrhA, we performed an EMSA assay with shortened
246 probes (I ~ IV). Sequences of probes I and II are identical to that of LBS I and LBS II
247 respectively, while sequences of probes III and IV are identical to regions of P_{cas} with
248 high and low affinity to LrhA respectively (Fig. 4b), as predicted by the SELEX

249 database[68]. We observed that LrhA bound probes I and II with high affinity, the probe
250 III with lower affinity, and the probe IV with the lowest affinity (Fig. 4b), confirming
251 that LrhA binds to both LBS I and LBS II.
252 The results above indicate that both LrhA and LeuO bind to LBS I and LBS II on P_{cas}
253 to regulate the expression of the *cas* operon (Fig. 4a and b). To know whether LBS I
254 and/or LBS II are essential to activate P_{cas} by LrhA and LeuO *in vivo*, we generated
255 P_{cas} containing disrupted LBS I and/or LBS II (Fig. 4c), and compared *in vivo*
256 activities of disrupted P_{cas} with that of P_{cas} FL in response to expression of LrhA and
257 LeuO. Over-expressing LrhA and LeuO increased the transcriptional activity of P_{cas}
258 FL by more than 3- and 8-fold, respectively (Fig. 4c). In contrast, the activity of P_{cas}
259 del LBS I in the Δ*hns* Δ*leuO* mutant expressing LrhA or LeuO was decreased to the
260 background level or 3.88-fold higher than the background level, respectively (Fig. 4c).
261 This observation indicates that LBS I is indispensable for activation of P_{cas} by LrhA,
262 and essential for full stimulation of P_{cas} by LeuO. Interestingly, the activity of P_{cas} del
263 LBS II was also remarkably reduced in the Δ*hns* Δ*leuO* mutant expressing either
264 LrhA or LeuO (Fig. 4c), revealing that LBS II was required for activation of P_{cas} by
265 both LrhA and LeuO. As expected, when both LBS I and LBS II were deleted, the
266 expression of LrhA or LeuO no longer stimulated the expression of the impaired P_{cas}
267 (Fig. 4c). Taken together, these data clearly show that both LBS I and LBS II are
268 essential for activation of P_{cas} by LrhA and LeuO *in vivo*.

269 DISCUSSION

270 In this study, we have addressed the important question of how the CRISPR-Cas
271 adaptive immunity is regulated in bacteria. Our work demonstrates that the LTTR
272 LrhA activates CRISPR-Cas adaptive immunity more efficiently at 37 ℃ than at
273 30 ℃ by promoting reciprocal interplay between interference and adaptation in *E. coli*.
274 Knowing how the endogenous CRISPR-Cas system is regulated under the
275 physiological condition would not only unravel its ecological and evolutionary role,
276 but also be a pre-requisite for devising strategies to steer the CRISPR-Cas system
277 towards MDR bacteria.

278 **LrhA triggers a positive feedback circuit between interference and primed**
279 **adaptation**

280 Early reports showed that primed adaptation was triggered by suboptimal
281 Cascade-protospacer interactions that could lead to weak interference[28,69,70]. However,
282 later studies reported that optimal Cascade-protospacer interactions also led to both
283 interference and primed adaptation, which was fueled by interference[31,66,71,72]. It
284 appears that the level of CRISPR immunity is determined by coordination of
285 interference and adaptation. In this study, we detected remarkably higher interference
286 and adaptation in the *lrhA*$^{+}$ strain than that in the *lrhA*$^{-}$ strain. Adaptation occurred
287 more frequently in the *lrhA*$^{+}$ *E. coli* strains harboring an intact *cas* operon and the
288 CRISPR-targeted plasmid (Fig. 2, and Supplementary Fig. S6), revealing that LrhA
289 can promote interference-driven spacer acquisition. Given that inactivation of *cas1*
290 and *cas2* remarkably reduced LrhA-stimulated CRISPR interference (Fig. 2h), we
291 propose that LrhA promotes the positive feedback circuit between CRISPR
292 interference and adaptation: cleavage of the CRISPR-targeted plasmid produces more
293 short DNA fragments for accelerating primed adaptation, which in turn enhances
294 clearance of the CRISPR-targeted plasmid (Fig. 5). Analysis of the acquired spacers
295 revealed an unequal distribution, indicating that certain sequences are preferentially
296 integrated as new spacers. We also noticed that most spacers were originated from the
297 same strands with a high preference for AAG PAM sequences (Fig. 2g and
298 Supplementary Table S3), matching traits of the primed adaptation process[28,30].
299 Compared with other regions on the CRISPR-targeted plasmid, protospacers were
300 mapped to encoding genes (i.e., *bla* and *dsRED*) and the replication origin with a
301 remarkably higher frequency (Fig. 2g), suggesting that unwinding of double-stranded
302 DNA during replication and transcription may facilitate the adaptation process.

303 **Temperature affects regulation of the CRISPR-Cas system by LrhA**

304 Previous work demonstrated that temperature regulates the CRISPR-Cas activity
305 in *Pseudomonas aeruginosa* by controlling growth rate[73]. Our study supports that
306 temperature affects the CRISPR-Cas adaptive immunity through controlling the
307 activity of P_{cas}, since LrhA promoted a higher rate of clearance of CRISPR-targeted

308 plasmid and stronger transcription of the *cas* operon at 37 ℃ than 30 ℃ in *E. coli* (Fig.
309 2 to 3). Considering that the amount of LrhA was not reduced in *E. coli* grown at
310 30 ℃ with regard to that at 37 ℃ (Supplementary Fig. S8), it seems that temperature
311 does not function by affecting the expression or stability of LrhA. Because the
312 deletion of *cas1* and *cas2* abolished the effect of temperature on regulation of
313 CRISPR interference, we conclude that temperature affected the CRISPR-Cas
314 adaptive immunity by influencing regulation of the positive feedback circuit between
315 interference and primed adaptation by LrhA. Since more frequent adaptation in the
316 *lrhA*$^{+}$ strain at 37 ℃ than at 30 ℃ (Fig. 2f) could be associated with weaker nuclease
317 activity of Cas3 at 37 ℃[66], LrhA may increase CRISPR interference with weak Cas3
318 by increasing the number of spacers matching sites on the targeted plasmid at 37 ℃.
319 Whereas, CRISPR interference with strong Cas3 at 30 ℃ could be unfavorable to
320 adaptation, restricting accumulation of spacers in the CRISPR array by LrhA.
321 Accordingly, we propose that, at the body temperature, LrhA may better coordinate
322 interference and adaptation to achieve maximal immunity, which is determined by the
323 combined effect of interference and adaptation, to reduce the risk of invading nucleic
324 acids.

325 **Regulation of the CRISPR-Cas system by LTTRs**

326 Both *in vivo* and *in vitro* evidence reveals that pleiotropic LTTRs LrhA and LeuO
327 activate the *cas* operon by binding to identical sites on P_{cas}. In contrast, the LTTR
328 ArgP was found to repress P_{cas}, showing diverse regulation of the CRISPR-Cas
329 system by LTTRs. In *Salmonella enterica*, transcription of the CRISPR-Cas system
330 was oppositely regulated by two LTTRs (i.e., LeuO and LRP) [74]. Considering the
331 widespread distribution of the type I CRISPR-Cas system (Supplementary Fig. S11),
332 it is possible that LTTR family proteins could extensively regulate CRISPR-Cas
333 systems in different bacteria. Although LeuO is normally considered as an antagonist
334 of H-NS, and activates gene transcription by relieving transcriptional suppression by
335 H-NS, we found that both LrhA and LeuO promoted the activity of P_{cas} in the Δ*hns*
336 Δ*leuO* mutants (Fig. 3b, 4c), indicating that they both regulated the *cas* operon

337 independent of H-NS. Nevertheless, exact roles of LrhA and LeuO on activating P_{cas}
338 remain unclear, awaiting further biochemical and structural analysis.
339 Despite similarities between LrhA and LeuO, they behaved remarkably differently in
340 regulating transcription of the *cas* operon and other genes as well. Most strikingly,
341 temperature showed a more pronounced impact on the regulation of the CRISPR-Cas
342 system by LrhA than that by LeuO (Fig. 3a and b). Although LeuO strongly
343 stimulated the *cas* operon at both body and environmental temperatures (Fig. 3b), it
344 stimulated weaker interference than LrhA did at the body temperature (Fig. 2b).
345 Strong stimulation of interference by LrhA could be the outcome of a reinforced cycle
346 of interference-driven adaptation and adaptation-promoted interference (Fig. 5). In
347 light of disrupting either of the two binding sites on P_{cas} abolished regulation by LrhA
348 while regulation of LeuO was abolished only when both of the two binding sites were
349 destroyed (Fig. 4c), the two regulators must interact with P_{cas} in different ways. Apart
350 from regulation of the CRISPR-Cas immunity, LrhA and LeuO showed remarkable
351 differences in controlling other aspects of bacterial physiology. Although inactivating
352 *lrhA* increased the swarming mobility by promoting transcription of the *flhDC* operon
353 in the presence or absence of LeuO, disrupting *leuO* failed to affect bacterial
354 swarming in both $lrhA^{+}$ and $lrhA^{-}$ strains (Supplementary Fig. S4). Phylogenetic
355 analysis revealed divergent evolution of LrhA and LeuO, which could belong to
356 distinct subfamilies and separately evolve in bacteria (Supplementary Fig. S9 and
357 S10). Moreover, regulation of the CRISPR-Cas system by LrhA or LeuO could be
358 evolved in response to different environmental cues, considering that expression of
359 LeuO can be activated by the heterodimer BglJ-RcsB[75], Cyanase regulator CynR[67],
360 and antibiotic responses regulator YdcI[67], while expression of LrhA is stimulated by
361 acid resistance-related gene *hdeD* [76].

362 METHODS

363 1. *Bacterial strains, plasmids, primers, growth conditions, and media*

364 Bacterial strains, plasmids, and primers used in this study are listed in Supplementary
365 Table S4, Table S5 and Table S6. *E. coli* gene-deletion mutants were constructed by

366 using a λ-RED recombination system expressed by the temperature-sensitive plasmid
367 pKD46[77]. Corresponding mutants were examined through PCR. Recombinant
368 plasmids expressing LrhA and other 10 TFs were constructed with a Transfer PCR
369 method[78]. Plasmids were isolated and purified with a plasmid isolation kit according
370 to the manufacturer's protocol (Axygen Biotech Co., Ltd.). *E. coli* cultures were
371 grown at 37 ℃ in LB broth containing 1% (wt/vol) tryptone, 0.5% (wt/vol) yeast
372 extract, and 1% (wt/vol) NaCl or on LB agar plates containing 1.5% (wt/vol) agar.
373 When evaluating the GFP/OD_{600} level or the interference/adaptation effect, cells were
374 grown in M9 minimal medium containing 61 mM $K_2HPO_4 \cdot 3H_2O$, 38.21 mM KH_2PO_4,
375 2.5 mM $MgSO_4$, 15.14 mM $(NH_4)_2SO_4$, 0.1% (wt/vol) tryptone, supplemented with
376 1% (wt/vol) glucose as the carbon source. When required, media were supplemented
377 with ampicillin (100 μg mL^{-1}), kanamycin (50 μg mL^{-1}), or chloramphenicol (25 μg
378 mL^{-1}). Arabinose was added for inducing gene expression in liquid cultures where
379 indicated. Cell growth was measured in a spectrophotometer (MD SpectraMax iD5 or
380 Biotek Synergy 2). All experiments were repeated independently at least three times
381 unless otherwise indicated.

382 **2. *pull-down assay***

383 To prepare samples for mass spectrometric analysis of proteins binding to P_{cas}, 8 pmol
384 biotinylated P_{cas} DNA fragment was coated with 100 μL streptavidin beads
385 (Invitrogen Dynabeads™ M-270) in the binding buffer A (10 mM Tris-HCl pH 7.5, 1
386 mM EDTA, 2 M NaCl) for 1 h at the room temperature. Biocytin, a derivative of
387 biotin, was used as the negative control. From a 5 mL culture of *E. coli hns*
388 deletion-mutant grown overnight at 37 ℃, proteins were extracted by sonication in
389 the binding buffer B (10 mM Tris-HCl pH 7.5, 1 mM EDTA, 50 mM NaCl, 0.4 mM
390 DTT and 10% glycerol), supplemented with protease inhibitor cocktail (Roche Co.,
391 Ltd.). The crude lysates were centrifuged at 15000×*g* for 10 minutes. The supernatant
392 was collected, pre-cleared by empty streptavidin beads, and then incubated with 50
393 μL P_{cas} DNA coated beads overnight at 4 °C under constant rotation (20 rpm). Beads
394 were washed 5 times with the binding buffer B, followed by washing 3 times with the
395 binding buffer B supplemented with 1 mg salmon sperm DNA, and finally washing 5

396 times with the binding buffer B to remove non-specific proteins. DNA binding
397 proteins were eluted in SDS sample loading buffer and loaded onto 10% SDS-PAGE,
398 followed by the mass-spectrometric analysis of the gel bands as described below.

399 **3. *Mass spectrometry analysis***

400 After 37℃ overnight in-gel digestion of proteins binding to P_{cas} with trypsin, peptides
401 were loaded onto a home-made reversed-phase analytical column (15-cm length, 75
402 μm i.d.), and analyzed with a gradient from 5% to 34% solvent B (0.1% formic acid
403 in 80% acetonitrile) over 40 min, 34% to 38% solvent B for 5 min, 38% to 90%
404 solvent B for 10 min, and then holding at 90% solvent B for 10 min, at a constant
405 flow rate of 300 nL/min on an EASY-nLC 1000 UPLC system. Peptides were
406 subjected to NSI source followed by tandem mass spectrometry (MS/MS) in Thermo
407 Scientific Orbitrap Fusion coupled online to the UPLC. Survey full-scan MS spectra
408 (m/z 350-1800) were acquired in the Orbitrap with resolution r of 70000 at m/z 400.
409 Mass spectrometry and analysis of the data were conducted by Micrometer Biotech
410 Company.

411 **4. *Quantification of gene transcription***

412 Plasmid pGLO-P_{cas}-*gfp* was used for monitoring the transcription of the *cas* operon,
413 by measuring the intensity of GFP fluorescence and cell optical density (OD_{600}) on a
414 microplate reader (MD, SpectraMax iD5), with a method that has previously been
415 described[50]. For Fig. 3a-c, *E. coli* BW25113 cells expressing pGLO-P_{cas} -*gfp* were
416 grown in M9 minimum medium at 30 ℃ or 37 ℃. For Fig. 4c, Plasmids pGLO-P_{cas}
417 -*gfp*, pGLO-P_{cas} del LBS I-gfp, pGLO-P_{cas} del LBS II-gfp, pGLO-P_{cas} del LBS
418 I&II-*gfp*, were transformed into the Δ*hns* Δ*leuO* mutant cells separately, for
419 measuring GFP/OD_{600} of cells grown in M9 minimum medium at 37 ℃.

420 **5. *Purification of LrhA Protein***

421 Full-length LrhA ORF with N terminal His-tag was cloned into the pET28A vector, to
422 generate pET28a-His-*lrhA*, which was transformed into *E. coli* BL21 (DE3). The
423 overnight culture was inoculated into 100 mL LB medium at a ratio of 1:100. When
424 the culture was grown to an OD_{600} of 0.4, expression of LrhA was induced with 0.5
425 mM IPTG (Beyotime, ST098) for 2 h. Cells were centrifuged at 8000 rpm for 5 min at

426 4 °C. The cell pellet was resuspended in PBS containing protease inhibitor and
427 sonicated, and the lysate was centrifuged at 12000×*g* for 5 min at 4 °C. His-LrhA
428 protein was purified by Ni-NTA Resin (ThermoFisher, 88222) in a gravity-flow
429 column, and the bound protein was eluted with PBS containing 250 mM imidazole.
430 The eluted protein was analyzed by SDS-PAGE, and dialyzed at 4°C in PBS with a
431 10 kDa dialysis tube (Millipore, UFC801096). Protein concentrations were
432 determined by the Bradford assay (Beyotime, P0006C).

433 ***6. Electrophoretic mobility shift assay (EMSA)***

434 EMSA was performed by using the LightShift Chemiluminescent EMSA kit
435 (ThermoFisher, 20148) according to the manual guide. P_{cas} (20 fmol) probes were
436 mixed with purified LrhA protein of different concentrations in the presence of
437 binding buffer (10 mM Tris-HCl pH 7.5, 50 mM KCl, 1 mM DTT, 2.5% glycerol, 1
438 mM EDTA). A Ctrl probe generated by PCR from the *lacZα* gene with primers P63
439 and P64 were used as control. The mixture was incubated at room temperature for 20
440 minutes, then separated by electrophoresis in 5% native polyacrylamide gels in
441 0.5×TBE buffer. Gels were visualized by SYBR Gold staining (ThermoFisher,
442 S11494). For Fig. 4b, bands were transferred to PVDF membrane using the semi-dry
443 transfer apparatus (Genscript) and visualized by Chemiluminescent Nucleic Acid
444 Detection Module (ThermoFisher, 89880). Images were collected with ChemiDoc™
445 XRS$^+$ (BioRad).

446 ***7. Plasmid loss assay***

447 The *E. coli* strains harboring the CRISPR-targeted plasmid pT (pDsRED-CR1) or the
448 CRISPR-non-targeted plasmid pNT (pDsRED) were grown overnight in LB culture
449 supplemented with ampicillin (100 μg mL^{-1}). The overnight grown culture was
450 washed and inoculated at a ratio of 2% into antibiotic-free LB culture, followed by
451 incubation at 30 ℃ or 37 ℃ with shaking. At intervals, the culture was serially
452 diluted and spread on the LB plate supplemented with or without ampicillin (100 μg
453 mL^{-1}). The number of cells maintained the plasmid was evaluated by comparing
454 colonies on the LB plate supplemented with or without ampicillin.

455 ***8. Spacer acquisition assay***

456 To monitor spacer acquisition, *E. coli* Δ*hns* Δ*leuO* and the Δ*hns* Δ*leuO* Δ*lrhA* strains
457 carrying pDsRED-CR1 or pDsRED were grown overnight in LB media supplemented
458 with ampicillin (100 μg mL^{-1}), then diluted to 1:50 times with antibiotic-free M9
459 media and growth was continued for 36 h at 30 ℃ or 37 ℃ with shaking. To monitor
460 CRISPR array expansion, cells from 200 μL of the culture were collected by
461 precipitation, washed thrice, and then resuspended in distilled water. These cells were
462 used as the template for PCR amplification of the CRISPR array I by using the primer
463 pair P65 (Adaptation-F) and P66 (Adaptation-R) as shown in Fig. 2e. All PCR
464 products were separated on 2% agarose gels to identify parental and expanded arrays
465 (parental array + 61bp). For sequencing newly acquired spacers, the expanded array
466 bands were excised, and corresponding DNA fragments were purified using a PCR
467 Clean-up kit (MN 740609.50), and ligated to T vectors (Takara, 6013).

468 ## Availability of data and materials

469 The raw data generated during the current study are available from the corresponding
470 authors on request. Source data are provided with this paper. Uncropped gels and
471 Western blots can be found in Supplementary Information. The mass spectrometry
472 proteomics data have been deposited to the ProteomeXchange Consortium
473 (http://proteomecentral.proteomexchange.org) via the iProX partner repository[79] with
474 the dataset identifier PXD036879.

475 ## COMPETING INTERESTS

476 We declare that we have no financial and personal relationships with other people or
477 organizations that can inappropriately influence our work, there is no professional or
478 other personal interest of any nature or kind in any product, service and/or company
479 that could be construed as influencing the position presented in, or the review of, the
480 manuscript entitled.

481

ACKNOWLEDGEMENT

This work was supported by the National Natural Science Foundation of China (grants 31670084 and 31100071), the Key Research and Development Program of Zhejiang Province (grant 2020C02031), and the Open Foundation of State Key Laboratory Cultivation Base of Hazard Factors and Risk Control of Quality and Safety of Agricultural Products (grant 2021DG700024-KF202105). We thank Prof. Shishen Du at Wuhan University and Dr. Yanmei Zhang at Hangzhou Medical College for scientific advice on this manuscript. We also thank Prof. Zhiyong Sun at Zhejiang University of Technology, Prof. Pengjun Zhang at Hangzhou Normal University, Ms. Minjia Shen at Université Paris-Saclay, Ms. Xia Yao at Zhejiang University of Technology, and all members of the Sun laboratory for critically reading the manuscript and helpful discussions.

496 # FIGURE LEGENDS

497 **Figure 1. Screen for new regulators modulating transcription of *cas* genes.**

498 (**a**) Schematic illustration of the CRISPR/Cas locus in *E. coli*. Repeats (diamonds) in
499 the CRISPR array are interspersed with 12 unique spacer sequences (rectangles). The
500 promoter of the *cas* operon (P_{cas}) is indicated by the black arrow. (**b**) The P_{cas} DNA
501 probe for pull-down assay contains a transcription start site (red letter), LeuO binding
502 site I and II (LBS I/II; purple bars), and H-NS binding site (HBS; yellow bar). (**c**)
503 Design of the pull-down proteomic experiment. A biotinylated probe (biotin-P_{cas} DNA)
504 was immobilized onto streptavidin beads, followed by incubation with extracts from *E.*
505 *coli* MC4100 Δ*hns* or BW25113 Δ*hns* before SDS-PAGE electrophoresis. (**d**)
506 SDS-PAGE gel electrophoresis of nontargeted biocytin (negative control, NT) or
507 biotin-P_{cas} DNA-binding proteins. NT or biotin-P_{cas} samples were digested in gel with
508 trypsin, and corresponding peptides were analyzed by mass spectrometry. An arrow
509 denotes the band corresponding to LrhA (34.593 kDa). (**e**) Peptides identified by mass
510 spectrometry (pink) were mapped to the amino acid sequence of LrhA. (**f**) Pull-down
511 assay of physical interaction between LrhA and P_{cas}. The biotinylated probe
512 (biotin-P_{cas} DNA) was immobilized onto streptavidin beads and incubated with
513 His-LrhA from cell extracts before (lane 3, input) and after (lane 2, P_{cas}) pull-down,
514 followed by western blot assay with antibody against His-tag. Nontargeted biocytin
515 (NT) was used as a negative control (lane 1). Arrow indicates the band of His-LrhA,
516 and the asterisk indicates a non-specific band. (**g**) Effects of 12 predicted TFs and
517 LeuO on the P_{cas} activity in *E. coli* BW25113 Δ*hns* Δ*leuO*. The cells were grown in
518 M9 medium supplemented with 10 mM arabinose, 100 μg/ml ampicillin and 25 μg/ml
519 chloramphenicol at 37 ℃ The P_{cas} activity was evaluated by GFP/OD_{600}, with the
520 relative expression level of Δ*hns* Δ*leuO* carrying empty vector pSU19 (Vector) as 1
521 arbitrary unit. All bars represent the mean, and error bars denote standard deviation.
522 Statistical significance was determined using one-way ANOVA with Dunnett's
523 multiple comparisons test. (**h**) Phylogenetic analysis of 9 HTH-type P_{cas}-binding TFs
524 from 5-8 different bacteria species.

525

526 **Figure 2. LrhA activates both CRISPR-Cas interference and adaptation.**

527 (**a**) Schematic illustration for evaluating the CRISPR-Cas interference activity by
528 plasmid loss assay. (**b**) Plasmid loss assay were performed in *E. coli* strains BW25113
529 Δ*hns* Δ*leuO* expressing GlpR, LeuO, SlyA, LrhA or ArgP. Cells carrying the pT
530 (CRISPR-targeted plasmid) or the pNT (CRISPR-non-targeted plasmid) were grown
531 in test tubes containing antibiotic-free M9 medium at 37 ℃ for 24 h, then serially
532 diluted for drop-plating onto LB agar plates supplemented with or without 100 μg
533 mL^{-1} ampicillin. (**c** and **d**) *E. coli* strains BW25113 Δ*hns* Δ*leuO* (*lrhA*$^{+}$), Δ*hns* Δ*leuO*
534 Δ*lrhA* (*lrhA*$^{-}$) or genomic *lrhA* complementation (*lrhA*^{c}) carrying the pT or the pNT
535 were grown in antibiotic-free M9 medium at 37 ℃ or 30 ℃. After 36 h growth,
536 plasmid loss was evaluated by drop-plating at 37 ℃ (**c**) or 30 ℃ (**d**). (**e**) Schematics
537 of the spacer acquisition assay in (**f** and **j**). During the adaptation process, a new
538 spacer (a yellow rectangle) can be inserted into the leader end of the CRISPR array.
539 PCR was performed to amplify the leader-spacer region using the primers matching
540 the leader and the second spacer, which were indicated as flagged arrows. (**f**)
541 Spacer-acquisition assay by PCR amplification of Δ*hns*Δ*leuO* (*lrhA*$^{+}$), Δ*hns* Δ*leuO*
542 Δ*lrhA* (*lrhA*$^{-}$) cells carrying the pT or the pNT plasmids, which were grown at 37 ℃
543 or 30 ℃ for 36 h. PCR products were electrophoresed on a 2% agarose gel and
544 imaged. Parental (P) and expanded bands (E) are indicated on the right while DNA
545 marker (M) positions are displayed on the left. Gels are representative of two
546 experiments yielding similar results. (**g**) Mapping of newly formed spacers on the pT
547 plasmid DNA. The DNA of the expanded array was sequenced by ligating purified
548 PCR products into T vectors. The position and orientation of the sequenced spacers
549 are marked on the pT plasmid map (blue arrows pointing clockwise and red arrows
550 pointing counterclockwise). Protospacers are numbered according to the strain from
551 which the spacers were sequenced, as listed in Supplementary Table 3. CR1 indicates
552 4 spacers targeted by the type I-E CRISPR-Cas system of *E. coli*. (**h-i**) Plasmid loss
553 assay of *E. coli* strains BW25113 Δ*hns* Δ*leuO* (*lrhA*$^{+}$), Δ*hns* Δ*leuO* Δ*lrhA* (*lrhA*$^{-}$),

554 Δ*hns* Δ*leuO* Δ(*cas1-cas2*) (*lrhA*$^{+}$Δ*cas1-2*) and Δ*hns* Δ*leuO* Δ*lrhA* Δ(*cas1-cas2*) (*lrhA*
555 $^{-}$Δ*cas1-2*) carrying the pT or the pNT, which were grown at 37 ℃ or 30 ℃ for 36 h.
556 (**j**) Spacer-acquisition assay by PCR amplification of Δ*hns*Δ*leuO* (*lrhA*$^{+}$), Δ*hns* Δ*leuO*
557 Δ*lrhA* (*lrhA* $^{-}$), Δ*hns* Δ*leuO* Δ(*cas1-cas2*) (*lrhA*$^{+}$Δ*cas1-2*) and Δ*hns* Δ*leuO* Δ*lrhA*
558 Δ(*cas1-cas2*) (*lrhA* $^{-}$ Δ*cas1-2*) cells carrying the pT, which were grown at 37 ℃ or
559 30 ℃ for 36 h. (**k**, upper panel) LrhA promotes the positive feedback circuit between
560 CRISPR interference and adaptation, which requires *cas1-2*. (**k**, lower panel) In
561 absence of cas1-2, LrhA showed a weak effect on interference since the adaptaion is
562 abolished.

563 **Figure 3. LrhA promotes transcription of the *cas* operon.**

564 (**a**) Effects of genomic *lrhA* on the P_{cas} activity in Δ*hns* Δ*leuO* grown in M9 medium
565 at 30 ℃ (left panel) or 37 ℃ (middle panel), with the relative expression level of
566 Δ*hns* Δ*leuO* of 24 h at 30℃ or 37℃ as 1 arbitrary unit. (**b**) Effects of LrhA or LeuO
567 expressed from the p15A derived plasmid pSU19 on the P_{cas} activity, indicated by
568 GFP/OD_{600}, were evaluated in BW25113 Δ*hns* Δ*leuO* mutants, which were grown in
569 M9 medium supplemented with 20 mM arabinose, 100 μg/ml ampicillin and 25 μg/ml
570 chloramphenicol at 30 ℃ (left) or 37 ℃ (middle). The relative expression level of *E.*
571 *coli* carrying empty vector pSU19 (Vector) was set as 1 arbitrary unit. (**c**) Effects of
572 genomic *lrhA* on the P_{cas} activity in Δ*hns* grown in M9 medium at 30 ℃ (left) or
573 37 ℃ (middle), with the relative expression level of Δ*hns* Δ*leuO* of 24 h incubation at
574 30 ℃ or 37 ℃ as 1 arbitrary unit. Mean values of at least three biological replicates
575 are shown as bars, and error bars indicate standard deviations. Data are shown as
576 means ± standard deviations (n = 4). Statistical significance was determined using
577 one-way ANOVA with Dunnett's multiple comparisons test (a, b) or an unpaired
578 two-tailed Student's t-test (c).

579 **Figure 4. Identification of LrhA binding sites on the promoter of the *cas* operon.**

580 (**a**, upper panel) Schematic illustration of the P_{cas} region for truncation analysis. LBS I
581 and LBS II indicate two DNA-binding sites of LeuO located upstream and
582 downstream of the transcriptional start site (TSS, black arrow) on P_{cas} (purple bars).

583 HBS indicates the DNA-binding site of the H-NS (yellow bar). (**a**, lower panel)
584 electrophoretic mobility shift (EMSA) assays of full-length or truncated P_{cas} DNA
585 fragments by LrhA. The P_{cas} probes including full-length P_{cas} (P_{cas} FL), P_{cas} with LBS
586 I deleted (P_{cas} del LBS I), P_{cas} with LBS II deleted (P_{cas} del LBS II) and P_{cas} with both
587 LBS I and LBS II deleted (P_{cas} del LBSI/II) were generated by PCR with primer P61
588 and P62. 20 fmol P_{cas} probes were separately incubated with a serial concentration of
589 purified His-LrhA, before EMSA assays with 5% native polyacrylamide gels (solid
590 arrow). A 175 bp *lacZα* fragment that was generated by PCR with primers P63 and
591 P64 was used as control (dashed arrow). (**b**, upper panel) Schematic of probes
592 matching the P_{cas} region for EMSA assay. DNA fragments "I" and "II" match LBS I
593 and LBS II respectively. DNA fragments "III" and "IV" match a region in between
594 LBS I and LBS II, and a region partially match downstream of LBS I respectively. (**b**,
595 lower panel) EMSA of DNA fragments "I" to "IV" by LrhA. Probes "I", "II", "III"
596 and "IV" were separately incubated with a serial concentration of purified His-LrhA
597 before EMSA assays with 5% native polyacrylamide gels. (**c**, upper panel) Schematic
598 illustration of DNA binding sites required for activating P_{cas} by LrhA and LeuO.
599 Transcriptional activities of full-length P_{cas}, P_{cas} del LBS I, P_{cas} del LBS II and P_{cas} del
600 LBS I/II were compared by using the P_{cas}-*gfp* reporter system. (**c**, lower panel) Effects
601 of disruption of LBS I and LBS II on activation of P_{cas} by LrhA. The P_{cas} activity was
602 evaluated by GFP/OD_{600}, with the relative expression level of Δ*hns* Δ*leuO* carrying
603 the empty vector as 1 arbitrary unit. The data are shown as means with standard
604 deviations from three independent experiments. Statistical significance was
605 determined using one-way ANOVA with Dunnett's multiple comparisons test.

606 **Figure 5. Schematic diagram of regulation of CRISPR-Cas immunity by LrhA in**
607 ***E. coli.*** LrhA binds to P_{cas} and activates transcription of the *cas* operon, increasing the
608 amount of the surveillance complex Cascade and the integrase Cas1-Cas2. LrhA not
609 only augments interference of CRISPR-targeted plasmid (pT), which is mediated by
610 Cascade and the nuclease Cas3, but also promotes interference-driven spacer
611 acquisition which is mediated by Cas1-Cas2, together with Cascade and Cas3.

612

613 # REFERENCES

614 1 Makarova, K. S. *et al.* Evolutionary classification of CRISPR-Cas systems: a burst of class 2
615 and derived variants. *Nat. Rev. Microbiol.* **18**, 67-83 (2020).
616 https://doi.org:10.1038/s41579-019-0299-x
617 2 Mohanraju, P. *et al.* Diverse evolutionary roots and mechanistic variations of the CRISPR-Cas
618 systems. *Science.* **353**, aad5147 (2016). https://doi.org:10.1126/science.aad5147
619 3 Hille, F. *et al.* The biology of CRISPR-Cas: backward and forward. *Cell.* **172**, 1239-1259
620 (2018). https://doi.org:10.1016/j.cell.2017.11.032
621 4 Koonin, E. V., Makarova, K. S. & Zhang, F. Diversity, classification and evolution of
622 CRISPR-Cas systems. *Curr. Opin. Microbiol.* **37**, 67-78 (2017).
623 https://doi.org:10.1016/j.mib.2017.05.008
624 5 Garneau, J. E. *et al.* The CRISPR/Cas bacterial immune system cleaves bacteriophage and
625 plasmid DNA. *Nature* **468**, 67-71 (2010). https://doi.org:10.1038/nature09523
626 6 Marraffini, L. A. & Sontheimer, E. J. CRISPR interference limits horizontal gene transfer in
627 staphylococci by targeting DNA. *Science.* **322**, 1843-1845 (2008).
628 https://doi.org:10.1126/science.1165771
629 7 Barrangou, R. *et al.* CRISPR provides acquired resistance against viruses in prokaryotes.
630 *Science.* **315**, 1709-1712 (2007). https://doi.org:10.1126/science.1138140
631 8 Horvath, P. *et al.* Diversity, activity, and evolution of CRISPR loci in *Streptococcus*
632 *thermophilus*. *J Bacteriol.* **190**, 1401-1412 (2008). https://doi.org:10.1128/jb.01415-07
633 9 Deveau, H. *et al.* Phage response to CRISPR-encoded resistance in *Streptococcus*
634 *thermophilus*. *J Bacteriol.* **190**, 1390-1400 (2008). https://doi.org:10.1128/jb.01412-07
635 10 Amitai, G. & Sorek, R. CRISPR-Cas adaptation: insights into the mechanism of action. *Nat.*
636 *Rev. Microbiol.* **14**, 67-76 (2016). https://doi.org:10.1038/nrmicro.2015.14
637 11 Lee, H. & Sashital, D. G. Creating memories: molecular mechanisms of CRISPR adaptation.
638 *Trends Biochem Sci.* **47**, 464-476 (2022). https://doi.org:10.1016/j.tibs.2022.02.004
639 12 Levy, A. *et al.* CRISPR adaptation biases explain preference for acquisition of foreign DNA.
640 *Nature* **520**, 505-510 (2015). https://doi.org:10.1038/nature14302
641 13 Sternberg, S. H., Richter, H., Charpentier, E. & Qimron, U. Adaptation in CRISPR-Cas
642 systems. *Mol. Cell* **61**, 797-808 (2016). https://doi.org:10.1016/j.molcel.2016.01.030
643 14 Patterson, A. G., Yevstigneyeva, M. S. & Fineran, P. C. Regulation of CRISPR-Cas adaptive
644 immune systems. *Curr. Opin. Microbiol.* **37**, 1-7 (2017).
645 https://doi.org:10.1016/j.mib.2017.02.004
646 15 Shivram, H., Cress, B. F., Knott, G. J. & Doudna, J. A. Controlling and enhancing CRISPR
647 systems. *Nat. Chem. Biol.* **17**, 10-19 (2021). https://doi.org:10.1038/s41589-020-00700-7
648 16 Pacesa, M. *et al.* R-loop formation and conformational activation mechanisms of Cas9. *Nature*
649 **609**, 191-196 (2022). https://doi.org:10.1038/s41586-022-05114-0
650 17 Xiao, Y. *et al.* Structure basis for directional R-loop formation and substrate handover
651 mechanisms in type I CRISPR-Cas system. *Cell.* **170**, 48-60 (2017).
652 https://doi.org:10.1016/j.cell.2017.06.012
653 18 Selle, K. & Barrangou, R. Harnessing CRISPR-Cas systems for bacterial genome editing.
654 *Trends Microbiol.* **23**, 225-232 (2015). https://doi.org:10.1016/j.tim.2015.01.008
655 19 Baumann, K. Genome editing: CRISPR-Cas becoming more human. *Nat. Rev. Mol. Cell. Biol.*

656 **18**, 591 (2017). https://doi.org:10.1038/nrm.2017.84
657 20 Stella, S., Alcón, P. & Montoya, G. Class 2 CRISPR-Cas RNA-guided endonucleases: Swiss
658 Army knives of genome editing. *Nat. Struct. Mol. Biol.* **24**, 882-892 (2017).
659 https://doi.org:10.1038/nsmb.3486
660 21 Wang, J. Y., Pausch, P. & Doudna, J. A. Structural biology of CRISPR-Cas immunity and
661 genome editing enzymes. *Nat. Rev. Microbiol.* **20**, 641-656 (2022).
662 https://doi.org:10.1038/s41579-022-00739-4
663 22 Bikard D, E. C., Jiang W, et al. Exploiting CRISPR-Cas nucleases to produce
664 sequence-specific antimicrobials. *Nat. Biotechnol.* **32**, 1146-1150 (2014).
665 https://doi.org:10.1038/nbt.3043
666 23 Citorik RJ, M. M., Lu TK. Sequence-specific antimicrobials using efficiently delivered
667 RNA-guided nucleases. *Nat. Biotechnol.* **32**, 1141-1145 (2014).
668 https://doi.org:10.1038/nbt.3011
669 24 Kiga K, T. X., Ibarra-Chavez R, et al. Development of CRISPR-Cas13a-based antimicrobials
670 capable of sequence-specific killing of target bacteria. *Nat. Commun.* **11**, 2934 (2020).
671 https://doi.org:10.1038/s41467-020-16731-6
672 25 Selle K, F. J., Tuson H, et al. In vivo targeting of clostridioides difficile using phage-delivered
673 CRISPR-Cas3 antimicrobials. *mBio* **11**, e00019-00020 (2020). https://doi.org:10.1128/mBio
674 26 Rosenblum D, G. A., Kedmi R, et al. CRISPR-Cas9 genome editing using targeted lipid
675 nanoparticles for cancer therapy. *Sci. Adv.* **6**, eabc9450 (2020).
676 27 Neil, K. *et al.* High-efficiency delivery of CRISPR-Cas9 by engineered probiotics enables
677 precise microbiome editing. *Mol. Syst. Biol.* **17**, e10335 (2021).
678 https://doi.org:10.15252/msb.202110335
679 28 Datsenko, K. A. *et al.* Molecular memory of prior infections activates the CRISPR/Cas
680 adaptive bacterial immunity system. *Nat. Commun.* **3**, 945 (2012).
681 https://doi.org:10.1038/ncomms1937
682 29 Fineran, P. C. & Charpentier, E. Memory of viral infections by CRISPR-Cas adaptive immune
683 systems: acquisition of new information. *Virology.* **434**, 202-209 (2012).
684 https://doi.org:10.1016/j.virol.2012.10.003
685 30 Swarts, D. C., Mosterd, C., van Passel, M. W. & Brouns, S. J. CRISPR interference directs
686 strand specific spacer acquisition. *PloS ONE.* **7**, e35888 (2012).
687 https://doi.org:10.1371/journal.pone.0035888
688 31 Semenova, E. *et al.* Highly efficient primed spacer acquisition from targets destroyed by the
689 *Escherichia coli* type I-E CRISPR-Cas interfering complex. *Proc. Natl Acad. Sci. USA.* **113**,
690 7626-7631 (2016). https://doi.org:10.1073/pnas.1602639113
691 32 Vale, P. F. *et al.* Costs of CRISPR-Cas-mediated resistance in *Streptococcus thermophilus*.
692 *Proc Biol Sci* **282**, 20151270 (2015). https://doi.org:10.1098/rspb.2015.1270
693 33 Jiang, W. *et al.* Dealing with the evolutionary downside of CRISPR immunity: bacteria and
694 beneficial plasmids. *PLoS Genet.* **9**, e1003844 (2013).
695 https://doi.org:10.1371/journal.pgen.1003844
696 34 Stern, A., Keren, L., Wurtzel, O., Amitai, G. & Sorek, R. Self-targeting by CRISPR: gene
697 regulation or autoimmunity? *Trends Genet.* **26**, 335-340 (2010).
698 https://doi.org:10.1016/j.tig.2010.05.008
699 35 Vercoe, R. B. *et al.* Cytotoxic chromosomal targeting by CRISPR/Cas systems can reshape

700 bacterial genomes and expel or remodel pathogenicity islands. *PLoS Genet.* **9**, e1003454
701 (2013). https://doi.org:10.1371/journal.pgen.1003454
702 36 Musharova, O. *et al.* Systematic analysis of Type I-E *Escherichia coli* CRISPR-Cas PAM
703 sequences ability to promote interference and primed adaptation. *Mol. Microbiol.* **111**,
704 1558-1570 (2019). https://doi.org:10.1111/mmi.14237
705 37 Blosser, T. R. *et al.* Two distinct DNA binding modes guide dual roles of a CRISPR-Cas
706 protein complex. *Mol. Cell* **58**, 60-70 (2015). https://doi.org:10.1016/j.molcel.2015.01.028
707 38 Redding, S. *et al.* Surveillance and processing of foreign DNA by the *Escherichia coli*
708 CRISPR-Cas system. *Cell* **163**, 854-865 (2015). https://doi.org:10.1016/j.cell.2015.10.003
709 39 Redding, S. *et al.* Surveillance and processing of foreign DNA by the *Escherichia coli*
710 CRISPR-Cas system. *Cell.* **163**, 854-865 (2015). https://doi.org:10.1016/j.cell.2015.10.003
711 40 Xiao, Y., Luo, M., Dolan, A. E., Liao, M. & Ke, A. Structure basis for RNA-guided DNA
712 degradation by Cascade and Cas3. *Science.* **361**, eaat0839 (2018).
713 https://doi.org:10.1126/science.aat0839
714 41 van Erp, P. B. *et al.* Mechanism of CRISPR-RNA guided recognition of DNA targets in
715 *Escherichia coli*. *Nucleic Acids Res.* **43**, 8381-8391 (2015).
716 https://doi.org:10.1093/nar/gkv793
717 42 Nunez, J. K., Lee, A. S., Engelman, A. & Doudna, J. A. Integrase-mediated spacer acquisition
718 during CRISPR-Cas adaptive immunity. *Nature* **519**, 193-198 (2015).
719 https://doi.org:10.1038/nature14237
720 43 Jackson, R. N. *et al.* Crystal structure of the CRISPR RNA-guided surveillance complex from
721 *Escherichia coli*. *Science.* **345**, 1473-1479 (2014). https://doi.org:10.1126/science.1256328
722 44 Sinkunas, T. *et al.* Cas3 is a single-stranded DNA nuclease and ATP-dependent helicase in the
723 CRISPR/Cas immune system. *EMBO J.* **30**, 1335-1342 (2011).
724 https://doi.org:10.1038/emboj.2011.41
725 45 Semenova, E. *et al.* Interference by clustered regularly interspaced short palindromic repeat
726 (CRISPR) RNA is governed by a seed sequence. *Proc. Natl Acad. Sci. USA.* **108**,
727 10098-10103 (2011). https://doi.org:10.1073/pnas.1104144108
728 46 . (!!! INVALID CITATION !!!).
729 47 Makarova, K. S., Zhang, F. & Koonin, E. V. SnapShot: Class 1 CRISPR-Cas Systems. *Cell.*
730 **168**, 946-946 (2017). https://doi.org:10.1016/j.cell.2017.02.018
731 48 Westra, E. R. *et al.* H-NS-mediated repression of CRISPR-based immunity in *Escherichia coli*
732 K12 can be relieved by the transcription activator LeuO. *Mol. Microbiol.* **77**, 1380-1393
733 (2010). https://doi.org:10.1111/j.1365-2958.2010.07315.x
734 49 Mitic, D., Radovcic, M., Markulin, D. & Ivancic-Bace, I. StpA represses CRISPR-Cas
735 immunity in H-NS deficient *Escherichia coli*. *Biochimie* **174**, 136-143 (2020).
736 https://doi.org:10.1016/j.biochi.2020.04.020
737 50 Sun, D. *et al.* Histone-like nucleoid-structuring protein (H-NS) paralogue StpA activates the
738 Type I-E CRISPR-Cas system againstnatural transformation in *Escherichia coli*. *Appl.*
739 *Environ. Microbiol.* **86**, e00731-00720 (2020). https://doi.org:10.1128/aem.00731-20
740 51 Yang, C. D., Chen, Y. H., Huang, H. Y., Huang, H. D. & Tseng, C. P. CRP represses the
741 CRISPR/Cas system in *Escherichia coli*: evidence that endogenous CRISPR spacers impede
742 phage P1 replication. *Mol. Microbiol.* **92**, 1072-1091 (2014).
743 https://doi.org:10.1111/mmi.12614

744 52 Pul, U. *et al.* Identification and characterization of *E. coli* CRISPR-*cas* promoters and their
745 silencing by H-NS. *Mol. Microbiol.* **75**, 1495-1512 (2010).
746 https://doi.org:10.1111/j.1365-2958.2010.07073.x
747 53 Yosef, I., Goren, M. G., Kiro, R., Edgar, R. & Qimron, U. High-temperature protein G is
748 essential for activity of the *Escherichia coli* clustered regularly interspaced short palindromic
749 repeats (CRISPR)/Cas system. *Proc. Natl Acad. Sci. USA.* **108**, 20136-20141 (2011).
750 https://doi.org:10.1073/pnas.1113519108
751 54 Majsec, K., Bolt, E. L. & Ivančić-Baće, I. Cas3 is a limiting factor for CRISPR-Cas immunity
752 in *Escherichia coli* cells lacking H-NS. *BMC microbiology* **16**, 28 (2016).
753 https://doi.org:10.1186/s12866-016-0643-5
754 55 Patterson, A. G. *et al.* Quorum sensing controls adaptive immunity through the regulation of
755 multiple CRISPR-Cas systems. *Mol. Cell* **64**, 1102-1108 (2016).
756 https://doi.org:10.1016/j.molcel.2016.11.012
757 56 Fang, F. C. & Rimsky, S. New insights into transcriptional regulation by H-NS. *Curr. Opin.*
758 *Microbiol.* **11**, 113-120 (2008). https://doi.org:10.1016/j.mib.2008.02.011
759 57 Corbett, D., Bennett, H. J., Askar, H., Green, J. & Roberts, I. S. SlyA and H-NS regulate
760 transcription of the *Escherichia coli* K5 capsule gene cluster, and expression of *slyA* in
761 *Escherichia coli* is temperature-dependent, positively autoregulated, and independent of H-NS.
762 *J Biol Chem* **282**, 33326-33335 (2007). https://doi.org:10.1074/jbc.M703465200
763 58 Lithgow, J. K., Haider, F., Roberts, I. S. & Green, J. Alternate SlyA and H-NS nucleoprotein
764 complexes control *hlyE* expression in *Escherichia coli* K-12. *Mol. Microbiol.* **66**, 685-698
765 (2007). https://doi.org:10.1111/j.1365-2958.2007.05950.x
766 59 Curran, T. D. *et al.* Identification of new members of the *Escherichia coli* K-12 MG1655
767 SlyA regulon. *Microbiology (Reading)* **163**, 400-409 (2017).
768 https://doi.org:10.1099/mic.0.000423
769 60 Nguyen Le Minh, P. *et al.* Differential protein-DNA contacts for activation and repression by
770 ArgP, a LysR-type (LTTR) transcriptional regulator in *Escherichia coli*. *Microbiol Res* **206**,
771 141-158 (2018). https://doi.org:10.1016/j.micres.2017.10.009
772 61 Lehnen, D. *et al.* LrhA as a new transcriptional key regulator of flagella, motility and
773 chemotaxis genes in *Escherichia coli*. *Mol. Microbiol.* **45**, 521-532 (2002).
774 https://doi.org:10.1046/j.1365-2958.2002.03032.x
775 62 Sun, D. *et al.* *Escherichia coli* is naturally transformable in a novel transformation system.
776 *FEMS Microbiol Lett* **265**, 249-255 (2006). https://doi.org:10.1111/j.1574-6968.2006.00503.x
777 63 Sun, D. *et al.* Transforming DNA uptake gene orthologs do not mediate spontaneous plasmid
778 transformation in *Escherichia coli*. *J Bacteriol* **191**, 713-719 (2009).
779 https://doi.org:10.1128/jb.01130-08
780 64 Zhang, Y., Shi, C., Yu, J., Ren, J. & Sun, D. RpoS regulates a novel type of plasmid DNA
781 transfer in *Escherichia coli*. *PLoS One* **7**, e33514 (2012).
782 https://doi.org:10.1371/journal.pone.0033514
783 65 Sasnauskas, G. & Siksnys, V. CRISPR adaptation from a structural perspective. *Curr. Opin.*
784 *Microbiol.* **65**, 17-25 (2020). https://doi.org:10.1016/j.sbi.2020.05.015
785 66 Kunne, T. *et al.* Cas3-derived target DNA degradation fragments fuel primed CRISPR
786 adaptation. *Mol. Cell* **63**, 852-864 (2016). https://doi.org:10.1016/j.molcel.2016.07.011
787 67 Breddermann, H. & Schnetz, K. Activation of *leuO* by LrhA in *Escherichia coli*. *Mol.*

Microbiol. **104**, 664-676 (2017). https://doi.org:10.1111/mmi.13656

68 Ishihama, A., Shimada, T. & Yamazaki, Y. Transcription profile of *Escherichia coli*: genomic SELEX search for regulatory targets of transcription factors. *Nucleic Acids Res.* **44**, 2058-2074 (2016). https://doi.org:10.1093/nar/gkw051

69 Fineran, P. C. *et al.* Degenerate target sites mediate rapid primed CRISPR adaptation. *Proc. Natl Acad. Sci. USA.* **111**, E1629-1638 (2014). https://doi.org:10.1073/pnas.1400071111

70 Xue, C. *et al.* CRISPR interference and priming varies with individual spacer sequences. *Nucleic Acids Res.* **43**, 10831-10847 (2015). https://doi.org:10.1093/nar/gkv1259

71 Staals, R. H. *et al.* Interference-driven spacer acquisition is dominant over naive and primed adaptation in a native CRISPR-Cas system. *Nat. Commun.* **7**, 12853 (2016). https://doi.org:10.1038/ncomms12853

72 Cooper, L. A., Stringer, A. M. & Wade, J. T. Determining the Specificity of Cascade Binding, Interference, and Primed Adaptation In Vivo in the *Escherichia coli* Type I-E CRISPR-Cas System. *mBio* **9** (2018). https://doi.org:10.1128/mBio.02100-17

73 Høyland-Kroghsbo, N. M., Muñoz, K. A. & Bassler, B. L. Temperature, by controlling growth rate, regulates CRISPR-Cas activity in *Pseudomonas aeruginosa*. *mBio* **9**, e02184-02118 (2018). https://doi.org:10.1128/mBio.02184-18

74 Medina-Aparicio, L. *et al.* The CRISPR/Cas immune system is an operon regulated by LeuO, H-NS, and leucine-responsive regulatory protein in *Salmonella enterica* serovar Typhi. *J Bacteriol* **193**, 2396-2407 (2011). https://doi.org:10.1128/JB.01480-10

75 Stratmann, T., Pul, Ü., Wurm, R., Wagner, R. & Schnetz, K. RcsB-BglJ activates the *Escherichia coli leuO* gene, encoding an H-NS antagonist and pleiotropic regulator of virulence determinants. *Mol. Microbiol.* **83**, 1109-1123 (2012). https://doi.org:10.1111/j.1365-2958.2012.07993.x

76 Yamanaka, Y., Aizawa, S. I. & Yamamoto, K. The *hdeD* Gene Represses the Expression of Flagellum Biosynthesis via LrhA in *Escherichia coli* K-12. *J Bacteriol.* **204**, e0042021 (2022). https://doi.org:10.1128/jb.00420-21

77 Datsenko, K. A. & Wanner, B. L. One-step inactivation of chromosomal genes in *Escherichia coli* K-12 using PCR products. *Proc. Natl Acad. Sci. USA.* **97**, 6640-6645 (2000). https://doi.org:10.1073/pnas.120163297

78 Erijman, A., Dantes, A., Bernheim, R., Shifman, J. M. & Peleg, Y. Transfer-PCR (TPCR): a highway for DNA cloning and protein engineering. *J Struct Biol.* **175**, 171-177 (2011). https://doi.org:10.1016/j.jsb.2011.04.005

79 Ma, J. *et al.* iProX: an integrated proteome resource. *Nucleic Acids Res.* **47**, D1211-d1217 (2019). https://doi.org:10.1093/nar/gky869

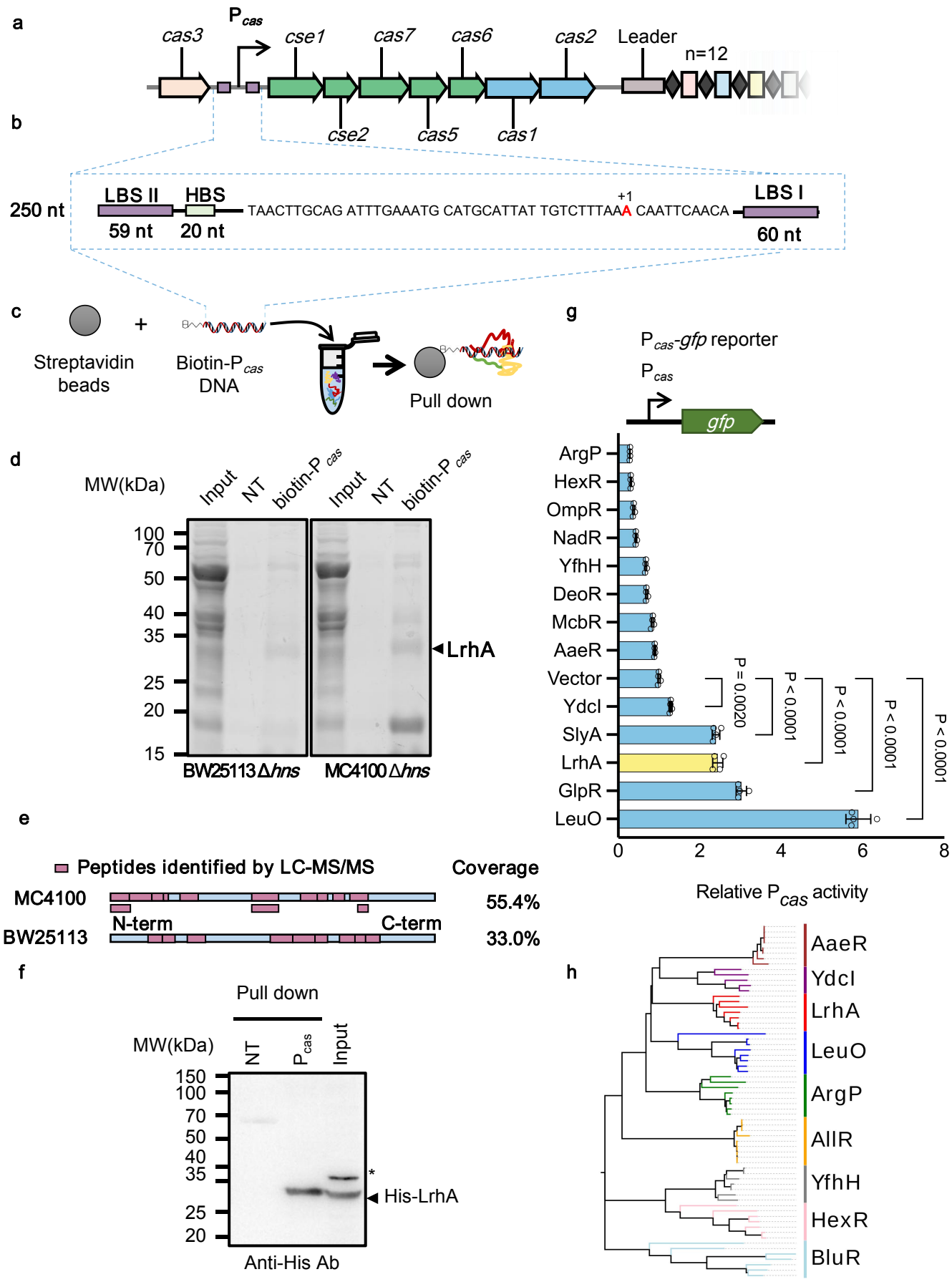
a
cas3
Pcas
cse1
cas7
cas6
cas2
Leader
n=12
cse2
cas5
cas1
b
250 nt
LBS II
HBS
TAACTTGCAG ATTTGAAATG CATGCATTAT TGTCTTTAAA CAATTCAACA
+1
LBS I
59 nt
20 nt
60 nt
c
Streptavidin beads
Biotin-Pcas DNA
Pull down
d
MW(kDa)
Input
NT
biotin-Pcas
100
70
50
40
35
25
20
15
LrhA
BW25113 Δhns
MC4100 Δhns
e
Peptides identified by LC-MS/MS
Coverage
MC4100
55.4%
BW25113
33.0%
N-term
C-term
f
Pull down
MW(kDa)
NT
Pcas
Input
150
100
70
50
40
35
25
20
His-LrhA
Anti-His Ab
g
Pcas-gfp reporter
Pcas
gfp
ArgP
HexR
OmpR
NadR
YfhH
DeoR
McbR
AaeR
Vector
YdcI
SlyA
LrhA
GlpR
LeuO
P = 0.0020
P < 0.0001
P < 0.0001
P < 0.0001
P < 0.0001
0
2
4
6
8
Relative Pcas activity
h
AaeR
YdcI
LrhA
LeuO
ArgP
AllR
YfhH
HexR
BluR

Figure 1

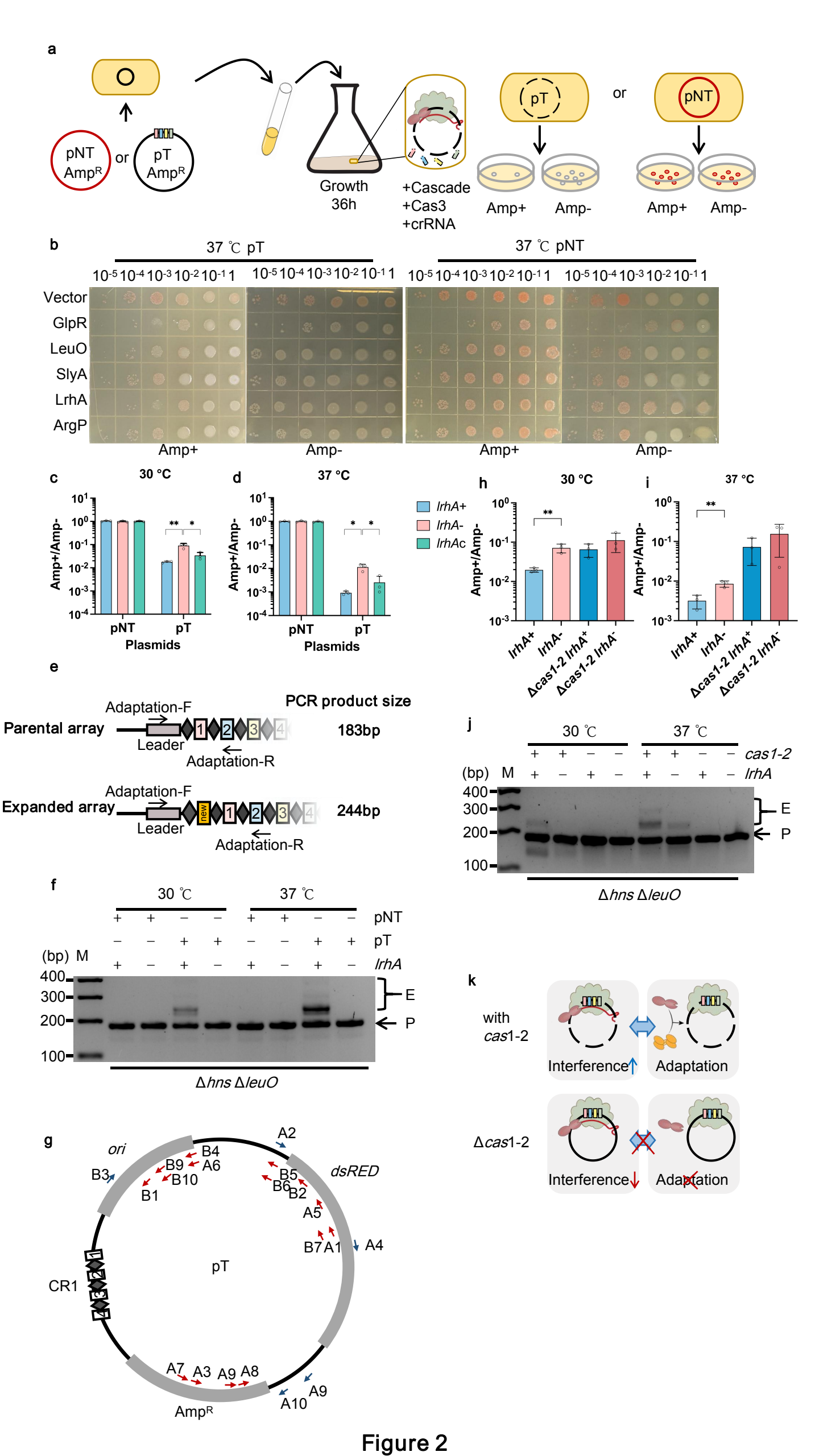
a
pNT AmpR
or
pT AmpR
Growth 36h
+Cascade +Cas3 +crRNA
pT
or
pNT
Amp+
Amp-
Amp+
Amp-
b
37 ℃ pT
37 ℃ pNT
10-5 10-4 10-3 10-2 10-1 1
Vector
GlpR
LeuO
SlyA
LrhA
ArgP
Amp+
Amp-
Amp+
Amp-
c
30 °C
d
37 °C
Amp+/Amp-
pNT
pT
Plasmids
lrhA+
lrhA-
lrhAc
h
30 °C
i
37 °C
lrhA+
lrhA-
Δcas1-2 lrhA+
Δcas1-2 lrhA-
e
PCR product size
Adaptation-F
Parental array
Leader
Adaptation-R
183bp
Adaptation-F
Expanded array
new
Leader
Adaptation-R
244bp
j
30 ℃
37 ℃
cas1-2
(bp) M
lrhA
400
300
200
100
E
P
ΔhnsΔleuO
f
30 ℃
37 ℃
pNT
pT
(bp) M
lrhA
400
300
200
100
E
P
ΔhnsΔleuO
k
with cas1-2
Interference
Adaptation
Δcas1-2
Interference
Adaptation
g
ori
B4
B9
A6
B3
B10
B1
A2
B5
B6
B2
dsRED
A5
B7
A1
A4
pT
CR1
A7
A3
A9
A8
A9
A10
AmpR

Figure 2

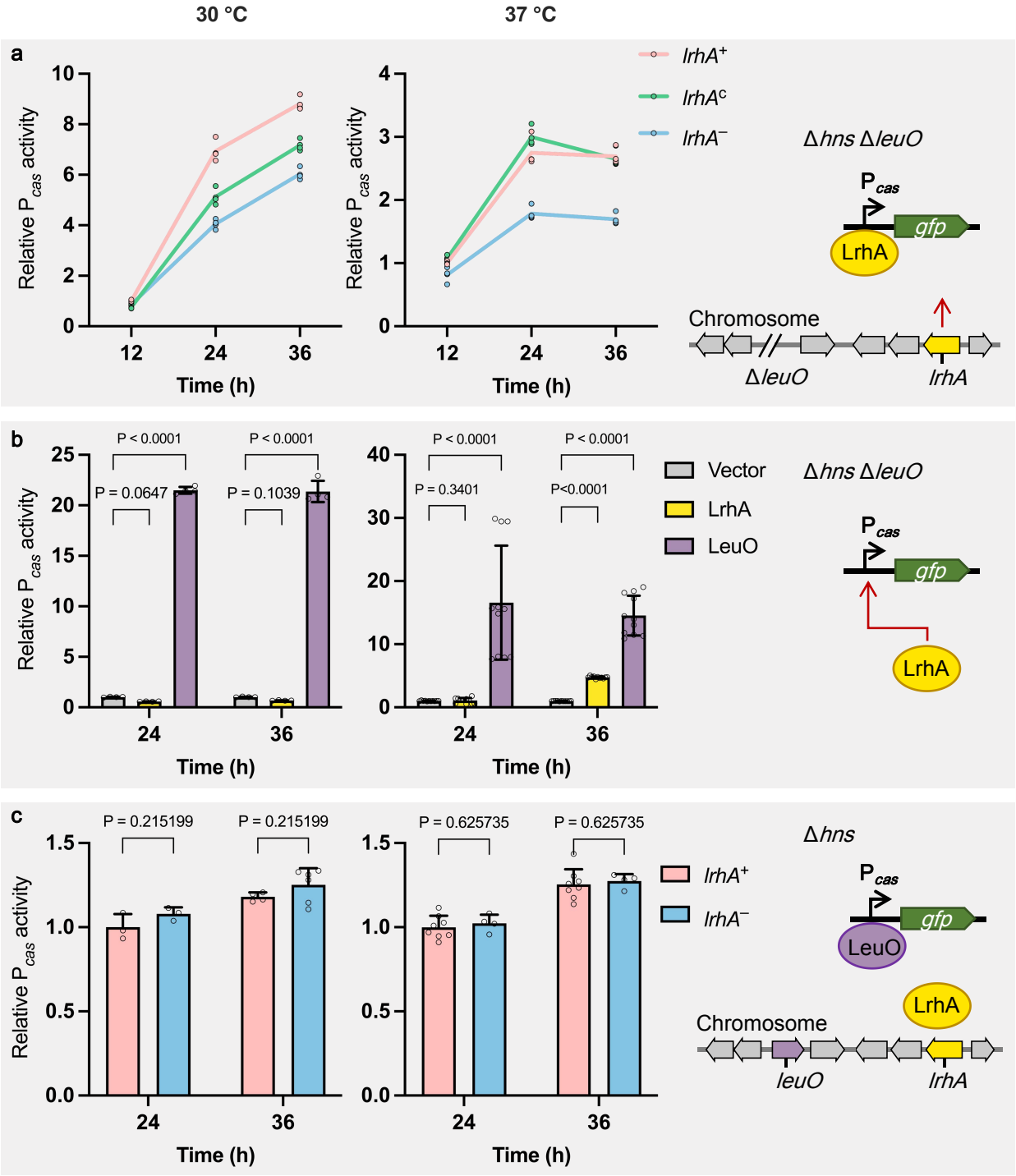
30 °C
37 °C
a
Relative P_{cas} activity
Time (h)
lrhA+
lrhAc
lrhA−
ΔhnsΔleuO
Pcas
gfp
LrhA
Chromosome
ΔleuO
lrhA
b
P < 0.0001
P = 0.0647
P = 0.1039
P = 0.3401
P<0.0001
Vector
LrhA
LeuO
c
P = 0.215199
P = 0.625735
Δhns
leuO

Figure 3

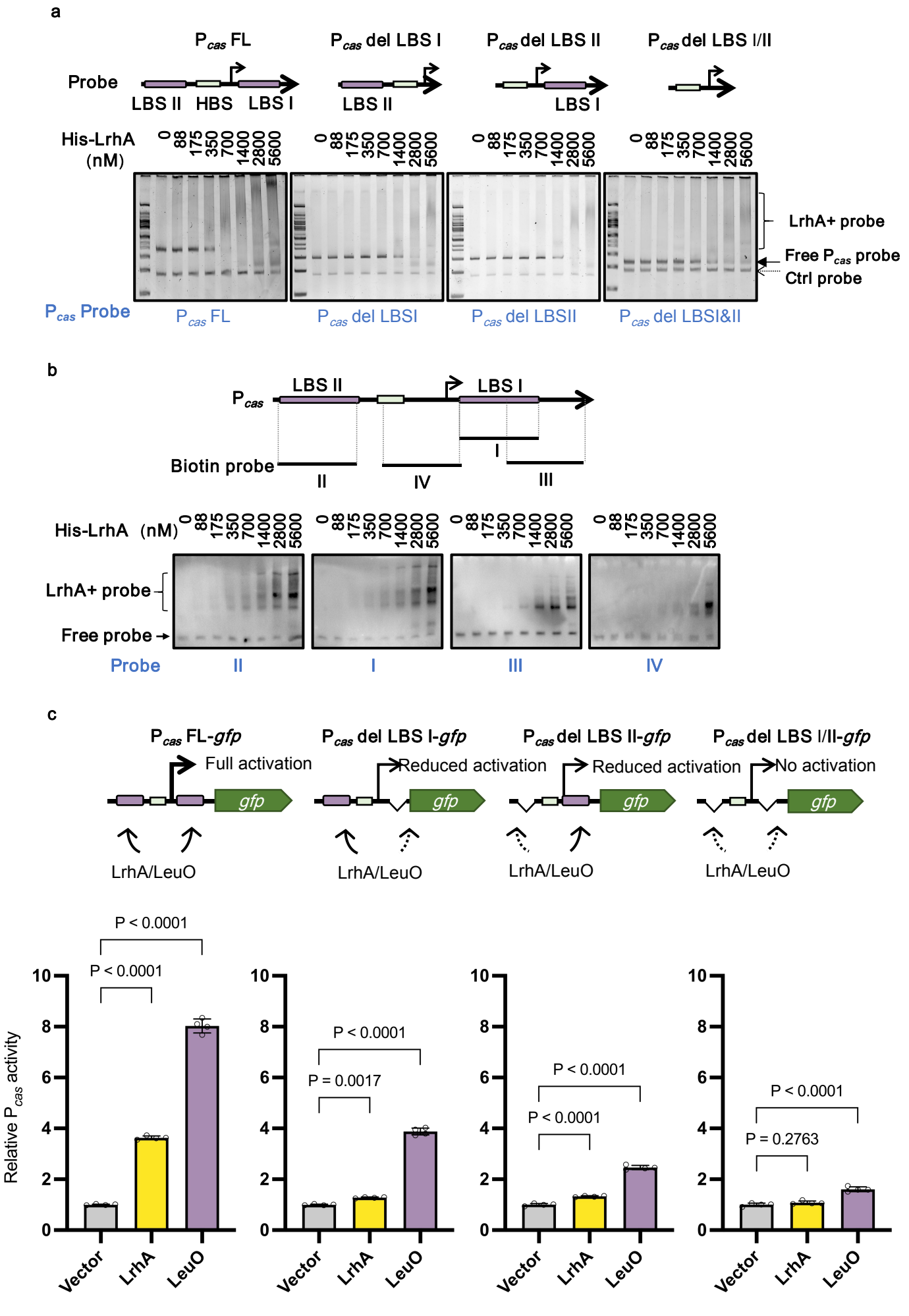
a
Pcas FL
Pcas del LBS I
Pcas del LBS II
Pcas del LBS I/II
Probe
LBS II
HBS
LBS I
His-LrhA (nM)
0 88 175 350 700 1400 2800 5600
LrhA+ probe
Free Pcas probe
Ctrl probe
Pcas Probe
Pcas FL
Pcas del LBSI
Pcas del LBSII
Pcas del LBSI&II
b
Pcas
LBS II
LBS I
Biotin probe
I
II
IV
III
His-LrhA (nM)
0 88 175 350 700 1400 2800 5600
LrhA+ probe
Free probe
Probe
II
I
III
IV
c
Pcas FL-gfp
Pcas del LBS I-gfp
Pcas del LBS II-gfp
Pcas del LBS I/II-gfp
Full activation
Reduced activation
Reduced activation
No activation
gfp
LrhA/LeuO
Relative Pcas activity
P < 0.0001
P < 0.0001
P < 0.0001
P = 0.0017
P < 0.0001
P < 0.0001
P < 0.0001
P = 0.2763
Vector
LrhA
LeuO

Figure 4

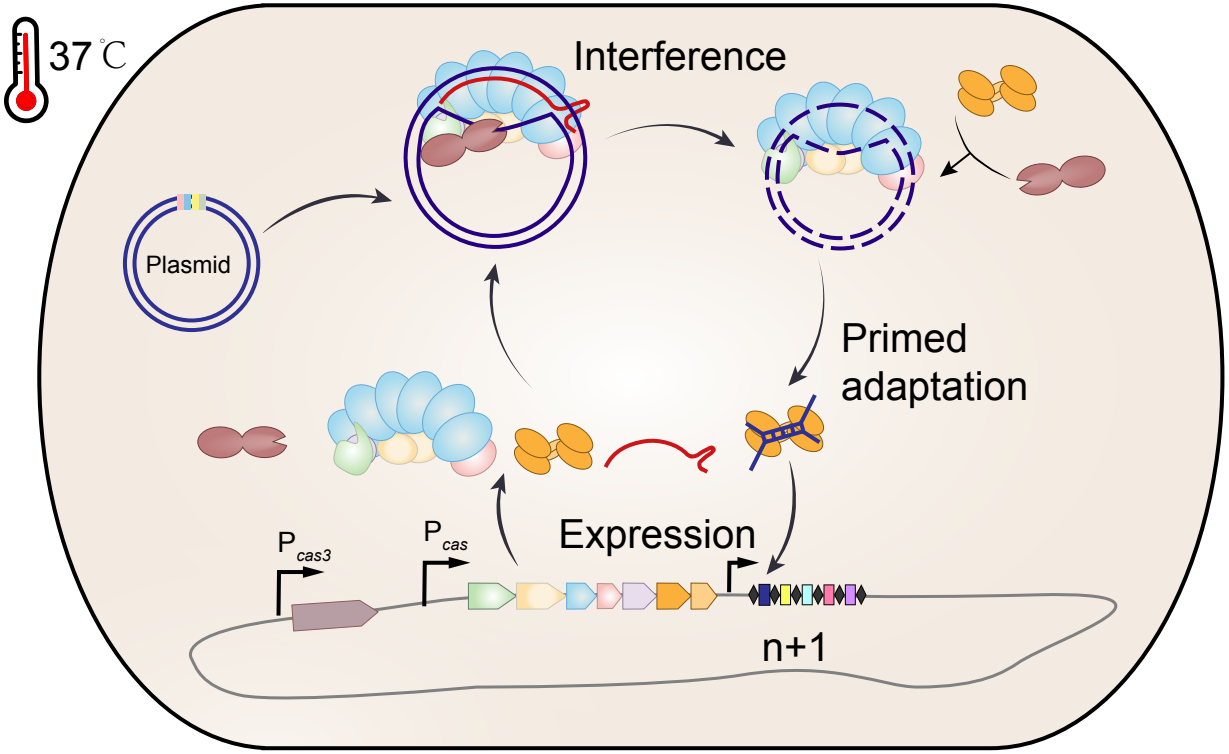
37 ℃
Interference
Plasmid
Primed
adaptation
Expression
P cas3
P cas
n+1

Figure 5